Iranian Journal of Fuzzy Systems

Volume 20, Number 2, (2023), pp. 33-55

Original paper

University of Sistan and Baluchestan

A controller design and analysis using asymmetry triangular cloud models

U. S. Pak[1], Y. N. Kim[2], J. Y. Kim[3] and J. S. Ri[4]

[1,2] *Faculty of Electronic and Automatic engineering, Kim Il Sung University, Pyongyang, Democratic Peoples Republic of Korea*
[3,4] *Postgraduate school, Kim Il Sung University, Pyongyang, Democratic Peoples Republic of Korea*

us.pak1207@ryongnamsan.edu.kp, auto4@ryongnamsan.edu.kp

Abstract

The cloud model is one of the mathematical tools that realize the transformation of quantitative information from qualitative data. Therefore, cloud model theory is widely used in computer science, reliability estimation, nonlinear function approximation, controller design, etc. In general, cloud controller design is known to use Gaussian membership clouds. However, it is computationally expensive because membership cloud computing is a nonlinear operation, and it has a disadvantage that it is difficult to decompose the structure of the controller. This paper proposes a new asymmetric triangular cloud model consisting of linear operations instead of Gaussian functions and, on this basis, develops a controller design method to approximate the output of the controlled plant to the desired value. Furthermore, it is demonstrated that the proposed controller is capable of stability analysis even if the mathematical model of the plant is not given, and it is validated by simulation of electrode up and down control of ultra-high power electric arc furnace and stabilization control of inverted pendulum.

Keywords: Fuzzy sets, asymmetry triangular membership cloud, cloud model, controller design, stability analysis.

1 Introduction

To deal with the fuzziness arising from the meaning of a human language or concept, L.A. Zadeh proposed the concept of fuzzy sets in 1965 [32].

The theory of fuzzy set has evolved very quickly, over half a century since its foundation, and the field of application has widened very rapidly [3, 4, 5, 14, 19, 26, 30, 34]. However, as theoretical research and industrial practice are widely disseminated, fuzzy set theory and fuzzy mathematics have faced continuous developmental challenges.

In [8], analysis and design of model-based fuzzy control systems was proposed. This was focused on stability analysis and controller design based on the so-called Takagi-Sugeno fuzzy models or fuzzy dynamic models. The fuzzy control algorithm consists of a set of heuristic control rules, and fuzzy sets and fuzzy logic are used, respectively, to represent linguistic terms and to evaluate the rules. The basic structure of a fuzzy control system consists of four conceptual components: knowledge base, fuzzification interface, inference engine, and defuzzification interface. Intelligent fuzzy controller for the tracking control of nonlinear hysteretic system was proposed in [2]. The control strategy of a nonlinear hysteretic system is investigated which can be used to systematically realize a stable fuzzy logic system. New closed-loop Back-propagation tuning is also proposed for the tuning of the fuzzy output membership functions to yield better tracking result. Finally, the controller synthesis is performed in a real-time environment. Neural network-based fuzzy controller was proposed in [28]. The dynamics of the neural network presented by linear differential inclusion (LDI) state-space representation, and control performance was achieved by using the parallel distributed compensation scheme. In [25], a parameter control method based on fuzzy logic was presented and the fuzzy logic approach was able to select any potential values for the parameter within a range without the potential values pre-defined by a user.

Corresponding Author: U. S. Pak
Received: November 2021; Revised: October 2022; Accepted: November 2022.
https://doi.org/10.22111/IJFS.2023.7555

The type-1 membership functions seem problematical, because a representation of fuzziness is made using membership grades that are themselves precise real numbers. The type-2 fuzzy set was introduced as an extension of the type-1 fuzzy set [1, 12, 20, 21, 22, 24, 31]. Thus, the concept of type-1 fuzzy sets was extended to type-2 fuzzy sets. Mendel (2003) and John introduced the new terminology to distinguish between the type-1 and type-2 membership functions, by which they represented the type-2 membership function in vertical-slice and wavy-slice manners respectively. The type-2 fuzzy set theory can be said to be a fuzzy set with fuzzy membership, i. e., the membership of the fuzzy set is defined as a continuous value between 0 to 1, i. e, a fuzzy number between 0 to 1, not one value, and the fuzzy inference method based on it. Based on the wavy-slice representation, they also proposed the concept of embedded fuzzy sets, which justifies the modelling capability of type-2 fuzzy sets and fuzzy logic systems for handling uncertainty. Mitchell ranked the type-2 fuzzy numbers by ranking the embedded type-1 fuzzy numbers associated with different weights. The type-2 fuzzy set theory doesn't represent the stochastic nature of the fuzzy set by several people, so it described the background of cloud mode theory which reflects fuzziness and stochastic nature [3, 16, 17, 18, 24, 27, 33]. The membership function once enters the world of correct mathematics after a person assumes and represents a correct numerical value, so membership cloud theory is proposed and then the definition of Gaussian membership cloud and cloud inference methods based on it [24]. In the last few years, there has been much work concerned with this theory, such as data mining [3], qualitative evaluation [27], pervasive computer [17], and so forth [1, 12]. In [6], cloud-model-based genetic algorithm was proposed, where use cloud model to adaptively tune the probabilities of crossover and mutation depending on the fitness values of solutions. Because normal cloud model has the properties of randomness and stable tendency. The method of combination of cloud model and neural network to find knowledge from imperfect data in Intelligent Decision Support System is proposed in [34]. The cloud is used to depict the imperfect data by group decision. In the following, attribution generation based on loud model or grey cloud model is used to generate the upper concept layer. In this step the cloud model depicting the imperfect data is classified into the concept layer that is proximal to itself according to distance between two cloud models. Specially, in the field of intelligence control, it has been successfully applied to balance one-, two- and three-link inverted pendulum system driven by single motors showing different balancing patterns and some robustness [11, 27].

A cloud model-based controller which needs no mathematical models of plant is presented reference [10, 18, 29, 35] proposed the controller design methods using Gaussian cloud model.

In these methods, equations of the membership cloud curve are nonlinear and the complexity of the calculation is very high because they have nonlinear and exponential nature, so it is difficult to analyse the decomposition structure of the controller and, as a result, the stability analysis of the closed-loop control system based on the Gaussian cloud model was not analytically validated but only with numerical simulations. One side, the cloudy normalized triangular fuzzy number (CNTFN) and Cloud Type Intuitionistic Dense Fuzzy number in the reference [13, 23] is the functions of two independent variables x and t, made good use of Economic order quantity (EOQ) model, which is composed of fuzziness measurement and inventory period time to build inventory model when the set-up cost, the average holding cost, the backorder cost, the raw material cost and the labor cost are characterized as fuzzy variables.

In this paper, an asymmetric triangular membership cloud consisting of linear operations instead of Gaussian membership clouds is newly proposed, and a controller design method based on it is developed, and a simple cloud controller structure is obtained, this controller is applied out for the control plant with a nonlinear uncertain model and stability analysis is carried.

The rest of the paper is proceeds as follows.

In Section 2, a novel asymmetric triangular cloud model is first proposed, and a controller design procedure using an asymmetric triangular cloud model to design the controller based on cloud inference without using the plant mathematical model is presented. Section 3 decomposes the structure of the controller using an asymmetric triangular cloud model. In Section 4, we consider the simplest controller structure of the triangular cloud controller because the controller structure using the triangular cloud model obtained in Section 3 is complex and it is difficult to deal with the stability analysis of the closed-loop system with that controller. Section 5 demonstrates the stability of the closed-cloud control system with the simplest cloud controller obtained in Section 4 using the Lyapunov function method to demonstrate that the controller using the proposed triangular cloud model ensures the stability of the system. In Section 6 we applies it to stabilization control of inverted pendulum and verified the effectiveness through computer simulation experiments. In Section 7, results analysis and future work are presented with the results obtained in the paper.

2 Controller design using an asymmetric triangular cloud model

We newly define an asymmetric triangular cloud whose membership curve is represented by an asymmetric triangular function rather than a Gaussian membership function.

The asymmetric triangular cloud model has following three characteristics.

I. The expected value Ex, the value corresponding to the center of gravity of the model in the defined area ($x = x_c = Ex, \mu(x_c) = 1$), $Ex = x_c$.

II. The entropy En_1 ,En_2, width of the curve of the model, reflect on degree to accept as a qualitative concept.

The equation of the curve of the model is defined by three parameters Ex, En_1, En_2.

$$\mu(x) = \begin{cases} 1 - \dfrac{x - En}{En_1}, & \text{if } (x - Ex) \geq En_1 \text{ and } x < Ex \\ 1 + \dfrac{x - En}{En_2}, & \text{if } (x - Ex) \leq En_2 \text{ and } x \geq Ex \\ 0, & \text{otherwise} \end{cases}$$

III. The hyperentropy- He, the entropy corresponding to the point M of the curve, ($x = Ex + \frac{2}{3}En, \mu = \frac{1}{3}$) , reflects on the degree of discrete of the membership cloud.

The controller with this cloud model is composed of the generator of the positive cloud, the cloud model projector, and the generator of the backward cloud. The generator of the positive cloud, corresponding to fuzzification interface, is a block that performs division of the cloud model for input variables and makes membership clouds for each division. At first, it performs division of the cloud model, which is the same as the course of fuzzy division. Next, membership cloud function for each division should be formulated and the course of it is shown by following details.

The algorithm to generate a positive asymmetric triangular cloud is following.

Step 1: Generate a normal distributed random variable x' that has two parameters of expectation Ex and entropy $(En_1 + En_2)/2$.

Step 2: Generate normal distribution random variable En_1' that has two parameters of expectation of expectation En_1 and entropy He.

Step 3: Generate normal distribution random variable En_2' that has two parameters of expectation of expectation En_2 and entropy He.

Step 4: Calculate $\mu_A(x')$ according to following equation.

$$\mu_A(x') = \begin{cases} 1 - \dfrac{x' - Ex}{En_1'}, & (x' - Ex) \geq En_1' \text{ and } x' < Ex \\ 1 + \dfrac{x' - Ex}{En_2'}, & (x' - Ex) \leq En_2' \text{ and } x' \geq Ex \\ 0, & \text{the other case.} \end{cases} \tag{1}$$

Step 5: Define $(x', \mu(x'))$ as a drop of cloud.

Step 6: Repeat step 1 to step 4 until drops of number k is generated.

If the asymmetric triangular membership cloud is expressed in a graph, it is shown in Fig. 1.

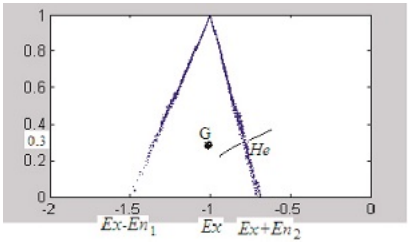

Figure 1: The characteristics of asymmetric triangular membership cloud

The comparison of our proposed asymmetric triangular membership cloud with previous fuzzy membership function and Gaussian membership cloud is shown in Fig. 2, 3, 4 and 5.

Fig. 2 shows the asymmetric triangular membership curves for the case of 1 expectation, 2 left entropy, 1.5 right entropy, and 0.05 hyperentropy, Fig. 3 shows the Gaussian membership clouds with 1 expectation, 0.6 entropy, and 0.05 hyperentropy, Fig. 4 shows the asymmetric triangular membership clouds for the case of zero hyperen-tropy, and Fig. 5 shows the asymmetric triangular fuzzy membership curves for the same central value and width.

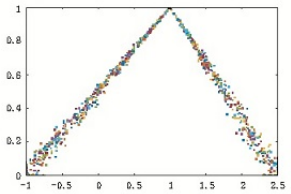

Figure 2: The asymmetric triangular membership cloud

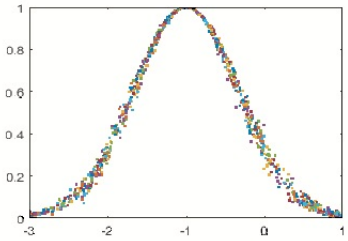

Figure 3: The symmetric Gaussian membership cloud

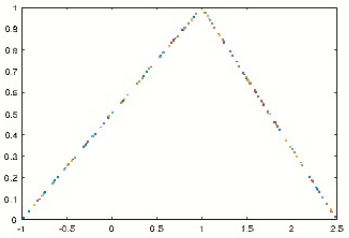

Figure 4: The asymmetric triangular membership cloud, case $He = 0$

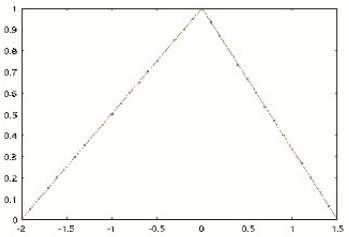

Figure 5: The asymmetric triangular fuzzy membership function

It can be seen from Fig. 4 that the membership and fuzzy membership curves for the case of zero hyperdispersion are the same. Fig. 6 shows the triangular membership cloud function graph when the number of clouds is 5.

Next, the cloud model projector has to be made up and it where assume x condition cloud model when the group of rules is already known by theory of the cloud model and generate the outputs to each input with combine of them consist of x condition cloud model and u conclusion cloud model.

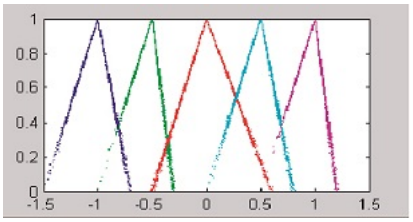

Figure 6: Triangular cloud function graph with 5 cloud divisions

x Condition cloud model is grouped into one degree of x condition cloud model, two degrees of x condition cloud model, compound degrees of x condition cloud model and n degrees of x condition cloud model by the order of the input vector, or premise of the rule.

Assume that the rules of one rule base are following.

$$\text{If } x = A_j, \text{ then } u = C_j, j = 1, 2, \cdots, m.$$

Then, x reflects on a condition of the control rule, which is called x condition cloud and u reflects on an inference conclusion according to condition x, where is called u conclusion cloud (or consequence of rule).

In the above rule, x is a variable of the cloud model and A_j is a member cloud, where $A_j = Tri(Ex_{xj}, En_{xj}, He_{xj}), j = 1, 2, \cdots, m$.

A means a triangular membership cloud with expected value Ex_x, entropy En_x, and hyper entropy He_x.

And, u is also a variable of the cloud model and Cj is a member cloud, where is $C_j = Tri(Ex_{uj}, En_{uj}, He_{uj})$. C means a triangular membership cloud with expected value Ex_u, entropy En_u, and hyper entropy He_u.

Figure 7 shows the one-dimensional cloud rule reasoning process.

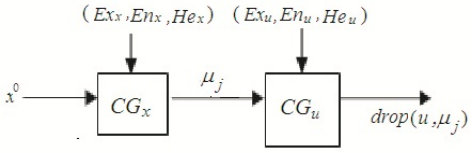

Figure 7: The one-dimensional cloud rule reasoning process

For instance, the process to generate first order x condition cloud is following.

Generate $\mu_A(x^0)$ for the certain input $x = x^0$ of the controller from the following equation.

$$\mu_A(x^0) = \begin{cases} 1 - \dfrac{x^0 - Ex}{En'_1}, & (x^0 - Ex) \geq En'_1 \text{ and } x^0 < Ex \\ 1 + \dfrac{x^0 - Ex}{En'_2}, & (x^0 - Ex) \leq En'_2 \text{ and } x^0 \geq Ex \\ 0, & \text{the other case} \end{cases} \tag{2}$$

Next, second order x condition cloud is expressed as the multiply of the group of drops of first order x condition cloud as the same case of normal cloud.

$$w_j^k = \begin{cases} \left(1 - \dfrac{x_1^0 - Ex_1}{En'_{11}}\right)\left(1 - \dfrac{x_2^0 - Ex_2}{En'_{21}}\right), & P_{condition} \\ \left(1 + \dfrac{x_1^0 - Ex_1}{En'_{12}}\right)\left(1 + \dfrac{x_2^0 - Ex_2}{En'_{22}}\right), & Q_{condition} \\ 0, \text{ the other case} \end{cases} \tag{3}$$

In the above equation,

$$En'_{11} = N(En_{11}, He), En'_{21} = N(En_{21}, He),\ En'_{12} = N(En_{12}, He), En'_{22} = N(En_{22}, He)$$
$$P_{condition} : (x_1^0 - Ex_1) \geq En'_{11} \text{ and } x_1^0 < Ex_1, \text{ and } (x_2^0 - Ex_2) \leq En'_{21} \text{ and } x_2^0 < Ex_2$$
$$Q_{condition} : (x_1^0 - Ex_1) \geq En'_{12} \text{ and } x_1^0 \geq Ex_1, \text{ and } (x_2^0 - Ex_2) \geq En'_{22} \text{ and } x_2^0 < Ex_2$$

where j is an index of the rule of cloud control and k is shown as the number of the cloud drops (Fig. 8).

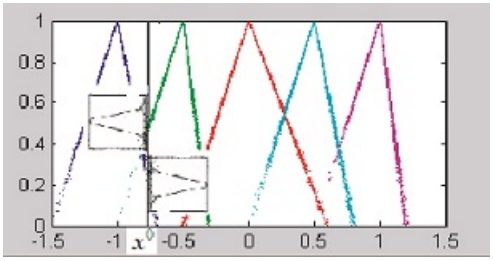

Figure 8: The generating process of the x conditional cloud models

When μ_j^k obtained in this way is inputted, the group of cloud drops-,$drop(u_j^k, \mu_j^k)$, where k is shown as the number of cloud drops, the output of u conclusion cloud based on first order rules, is outputted.

The process to generate u conclusion cloud is following.

It follows from the variables Ex_u - the expected value of consequence triangular membership cloud, En_u - the width of it and He_u - the entropy that determine

$$u_j^k = \begin{cases} Ex_u - (w_j^k - 1)En'_u, x < Ex_x \\ Ex_u + (w_j^k - 1)En'_u, x \geq Ex_x \end{cases} \tag{4}$$
$$En'_u = N(En_u, He_u).$$

In the above equation, u is equal u_j^k because u is presented as a group of k cloud drops for j^{th} rule.

This process is shown in Figure 9.

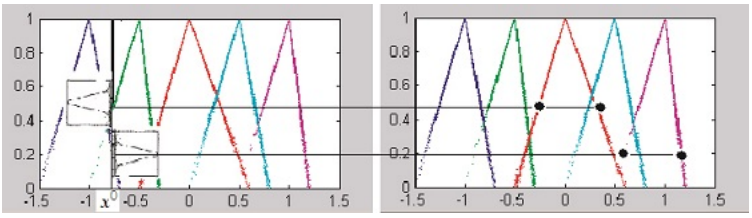

Figure 9: The generating process of a u conclusion cloud model

The generator of the backward cloud where is a process in order to calculate parameters Ex, En, and He of triangular membership cloud from the group of cloud drops obtained is presented as

$$Ex_{uj} = mean(u_j^k),\ u_j = Ex_u,\ u_j = \frac{\sum_{k=1}^{1000} w_j^k u_j^k}{1000}.$$

In the above equation, 1000 means the number of cloud droplets.

Finally, the output u is calculated by the weighting balance.

$$u = \frac{\sum_{j=1}^{m} w_j u_j}{\sum_{j=1}^{m} w_j}.$$

Example 2.1. *Consider the process of approximating the following nonlinear function using the proposed triangular membership cloud:* $y = \sin(x) + N(0, 0.05), x \in [-\pi/2, \pi/2]$

In the above equation, is a measure of uncertainty, representing a random number of Gaussian distributions with zero mean and 0.05 variance.

First, the parameters of the membership cloud curve for the input variable and the output variable are set as follows: the expected values of the asymmetric triangular membership cloud function of the preceding variables of the cloud inference rule as input variable are $[-\pi/2, -\pi/3, -\pi/4, -\pi/6, 0, \pi/6, \pi/4, \pi/3, \pi/2]$*, the left entropy and the right entropy value are set as* $[0, \pi/6, \pi/12, \pi/12, \pi/6, \pi/6, , \pi/12, \pi/12, \pi/12]$*,* $[\pi/6, \pi/12, \pi/12, \pi/6, \pi/6, , \pi/12, \pi/12, \pi/6, 0]$*, and the hyperentropy is set as 0.05 because the variance of noise is set as 0.05. The expected values of the single-point membership cloud function of the conclusion variable of the cloud inference law as the output variable were set to* $[-1, -0.86, -0.707, -0.5, 0, 0.5, 0.707, 0.86, 1]$.

The results obtained by the proposed method, fuzzy inference and Gaussian cloud inference method for the above parameters are shown in Fig. 10.

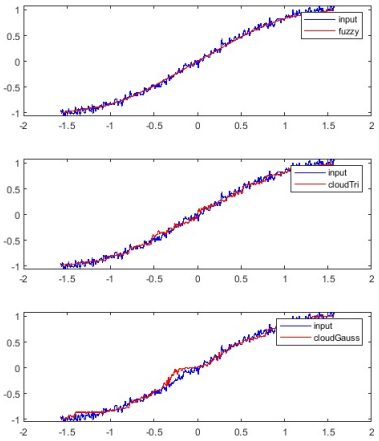

Figure 10: Results of approximating nonlinear functions by the proposed method, fuzzy inference and Gaussian cloud inference.

It can be seen from the figure that when approximated by fuzzy reasoning, there is no concern about the noise amplitude of the function to be approximated, but triangular or Gaussian cloud reasoning approximates the noise amplitude.

And we can see that the approximation result by triangular cloud inference is better than that by Gaussian cloud inference.

Example 2.2. *As an example of a triangular cloud controller, to verify the effectiveness of the simulation experiment, we consider the electrode lifting control of an ultra-high power electric arc furnace(UHP)* [9, 7].

The mathematical model of the plant for the electrode lifting control of the UHP furnace is expressed as.

$$Z = \frac{(X^2 + R_2^2)E_2}{-R_2(\beta L + \alpha) + \sqrt{(X^2 + R_2^2)E'^2_2 - X^2(\beta L + \alpha)}} \frac{15u}{s(0.1s + 1)}.$$

The physical quantities used in the mathematical modeling of an electric arc furnace shown in Tab. 1.

In the above equation, the voltage drop per arc length varies β *In the above equation, the voltage drop per arc length varies* $380V$ $430V(tap = 7)$ *in the melting stage,* $250V$ $300V(tap = 14)$ *in the oxidation stage and* $200V$ $220V(tap = 17)$ *in the reduction stage, Accordingly,* E'_2 *and* E_2 *is changed as follows.*

$$E'_2 = \frac{U_2}{\sqrt{3}}, \ E_2 = \sqrt{E'^2_2 - (X^2 - X_2^2) \cdot I^2}.$$

Table 1: The physical quantities used in the mathematical modeling of an electric arc furnace.

Symbol	Physical meaning	Unit
U_1	Primary phase voltage	V
$E_2^{'}$	Second-phase voltage that scales to the first side $E_2^{'} = U_1/\sqrt{3}k_b$	V
E_2	Second-phase voltage	V
k_b	Transform ratio of a furnace transformer. Following the transformer tap	
I	Arc current	A
U_a	Arc voltage	V
L	Arc length	mm
β	Voltage drop per arc length, Fusion step: gradually decrease from 12. Oxidation step:3.7, Reducing step:1.2	V/mm
α	Voltage enhancement at the anode and cathode of the electrode, $\alpha = 9$	V
X	Sum of the reactance of the primary and secondary circuits $X = (X_r + X_b)/k_b^2 + X_2$	Ω
X_r	Inductance of reactor, Following the reactor tap	Ω
X_b	Inductance of transformer	Ω
X_2	Total reactance of secondary circuit. 0.3×10^{-3}	Ω
R_2	Total resistance of the secondary circuit. 0.507×10^{-3}	Ω
Z	Impedance of secondary circuit. $Z = \sqrt{(R_a + R_2)^2 + X^2}$	Ω

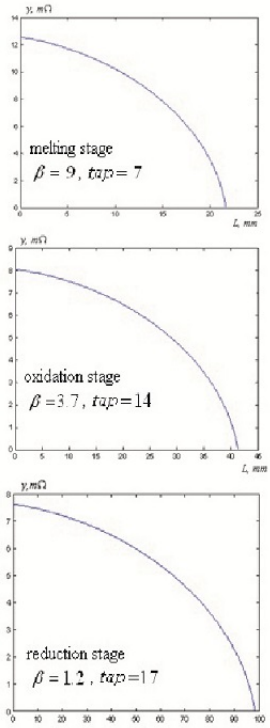

Figure 11: $L - y$ curve according to the melting stage

Drawing a $L-y$ curve according to the melting stage is shown in Fig. 11.

From the above figure, it can be seen that the dynamic characteristics of the plant vary drastically with the process stat. Therefore, control with the same control parameters during the melting process by electrode boost control in the ultra-high-power electric arc furnace cannot achieve the desired control effect, and should be applied a cloud PID control method that can change the control parameters depending on the melting stage and overcome uncertainty.

The configuration of the electrode step-up cloud PID control system of UHP furnace is shown in Fig. 12.

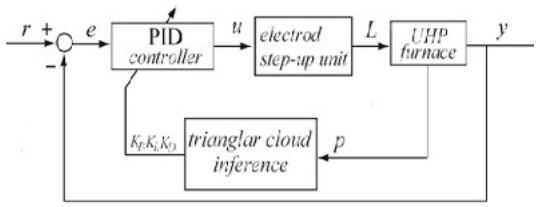

Figure 12: Configuration of the electrode step-up cloud PID control system of UHP furnace

In the figure, r is the target quantity, the set value of impedance when the active power applied to the UHP furnace is maximum, y is the impedance of the UHP furnace, u is the voltage applied to the hydraulic piston driving the electrode up and down in the UHP furnace, and e is the deviation of the target and control quantity, p is melting stage.

In order to ensure that the impedance of the UHP electric arc furnace is matched to the impedance set value, the process of varying the PID coefficients by triangular cloud inference is as follows.

- positive cloud generator

Since the error and error rate are considered as inputs of cloud controller and as output its PID coefficients, cloud partitioning and membership cloud generation for these input/output variables are performed as discussed in Section 2.

As seen earlier, the melting process of the UHP furnace varies with the melting stage, so sets the melting step as input of the cloud controller, the Pid coefficients as output.

the melting stage is set from 0 to 1, the range of PID coefficients respectively is set from 0 to 0.007, from 0 to 2.5, from 0 to 0.6 and the range of cloud I/O variables is set from 0 to 1 and so the cloud scale coefficients and scale coefficients are calculated as follows.

$$k_e = \frac{1-0}{1-0} = 1,\ k_{k_p} = \frac{0.0007-0}{1-0},\ k_{k_I} = \frac{2.5-0}{1-0},\quad k_{k_D} = \frac{0.6-0}{1-0}.$$

We use a symmetric triangular cloud for simplicity, and the membership cloud function of the premise and consequent variables is shown in Fig. 13 and 14. The hyper entropy He among the premise and consequent member cloud parameter values reflects uncertainty. The melting stage of the furnace in the UHP furnace vary according to the account the type of charge, value of charge, feeding of transmission, and the time of transmission, be considered as an uncertainty of the system, and so I/O variables hyper entropy He is set to be 0.03.

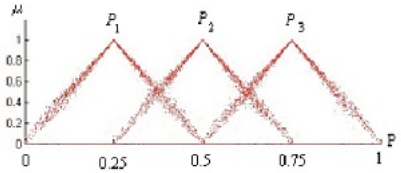

Figure 13: Membership cloud function of premise variable

Calculate the membership degree when the value is entered at the input of the cloud controller and the following

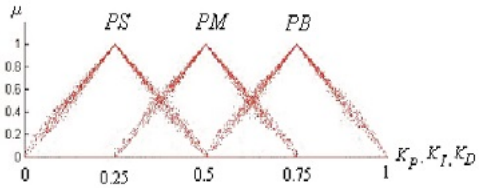

Figure 14: Membership cloud function of consequent variable

expression is shown in the following.

$$\mu_{P_i}^k(p^0) = \begin{cases} 1 - \left|\frac{p^0 - Ex_{p_i}}{En'_{p_i}}\right|, |p^0 - Ex_{p_i}| \le \left|En'_{p_i}\right| \\ 0, \ otherwise \end{cases}$$

$$En'_{p_i} = N(En_{p_i}, He_{p_i}).$$

where k represents the number of cloud drop i the index representing the number of partitions of the key member function, $N(En_{p_i}, He_{p_i})$ represents the random number of Gaussian distributions with mean En_{p_i} and variance He_{p_i}.

It can be seen that since the cloud controller input variables is own, it is the same as the upper one to calculate the goodness of fit according to the one-dimensional cloud map.

Then, according to the rule Tab. 2 of the cloud controller, we determine the membership cloud of the consequent variable PID and then determine the cloud droplet cluster.

When expected values consequent Membership cloud functions are Ex_{u_i}, entropies are En_{u_i}, hyper entropies are He_{u_i}, u condition cloud model is the following.

$$u_{lj}^k = \left\{ \begin{array}{l} Ex_{u_i} - (\mu_{P_i}^k - 1)En'_{u_i}, u_l < Ex_{u_l} \\ Ex_{u_i} + (\mu_{P_i}^k - 1)En'_{u_i}, u_l \ge Ex_{u_l} \end{array} \right\}$$

$$En'_{u_i} = N(En_{u_i}, He_{u_i}),\ l = K_P, K_I, K_D,\ j = 1, 2, 3,\ k = 1000.$$

The generator of the backward cloud where is a process in order to calculate parameters Ex, En and He of triangular

Table 2: The rules of K_P, K_I, K_D.

Step	K_P	K_I	K_D
P_1	PS	PS	PB
P_2	PM	PM	PM
P_3	PB	PB	PS

membership cloud from the group of cloud drops obtained is presented as

$$u_{lj} = \frac{\sum_{k=1}^{1000} \mu_{P_j}^k u_{lj}^k}{1000}.$$

In the above equation, 1000 means the number of cloud droplets.

Finally, the output K_P, K_I, K_D are calculated by the weighting balance.

$$K_P = u_1 = \frac{\sum_{j=1}^{3} \mu_{P_j} u_{1j}}{\sum_{j=1}^{3} \mu_{P_j}},\ K_I = u_2 = \frac{\sum_{j=1}^{3} \mu_{P_j} u_{2j}}{\sum_{j=1}^{3} \mu_{P_j}},\ K_D = u_3 = \frac{\sum_{j=1}^{3} \mu_{P_j} u_{3j}}{\sum_{j=1}^{3} \mu_{P_j}}.$$

The cloud PID control algorithm is expressed as follows.

$$u(k) = K_p \left[e(k) + \frac{T_c}{T_i} \sum_{i=0}^{k} e(i) + \frac{T_d}{T_c} (e(k) - e(k-1)) \right] = K_p e(k) + K_I T_c \sum_{i=0}^{k} e(i) + \frac{K_D}{T_c} \Delta e(k),$$

The block diagram and resulting curve for simulating of resistance control of UHP electric arc furnace by the proposed method, fuzzy control and Gaussian cloud control, are shown in Fig. 15, 16, and Fig. 17.

The block diagram and resulting curve for simulating of resistance control of UHP electric arc furnace are shown in Fig. 15.

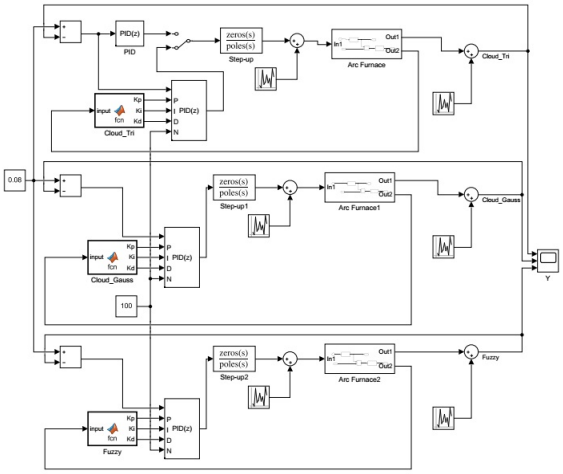

Figure 15: Block diagram for simulating of resistance control of UHP electric arc furnace

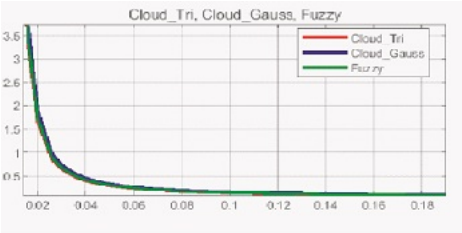

Figure 16: Resulting curve block diagram for simulating of resistance control of UHP electric arc furnace(case Noise-free)

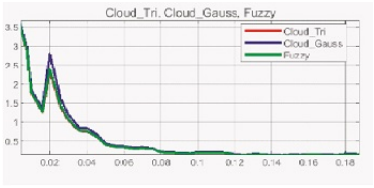

Figure 17: Resulting curve block diagram for simulating of resistance control of UHP electric arc furnace(case Noise)

From Fig. 16 and 17 , it can be seen that in the absence of noise (process uncertainty and measurement noise), the results of the proposed method, fuzzy control and Gaussian cloud control are similar, but in the presence of noise, the proposed method has a smaller overshoot and shorter transient time compared to the fuzzy control or Gaussian cloud control.

3 The structure analysis of the triangular cloud controller

The asymmetric triangular cloud controller presented in the previous section is a method of designing the controller based on expert knowledge without using the analytical model of the plant. Therefore, the stability analysis of a closed-loop system using an asymmetric triangular cloud controller is not mathematically validated and can only be explained by numerical simulations. In this section, the structural decomposition of the cloud controller is performed to perform the stability analysis of the previously designed cloud controller.

In order to analyses the Structure of the above cloud controller, suppose the input membership cloud functions crosses each other at their expectant value points and they are symmetric and have equal distributions.

For example, here shows a structure analysis of a 2 dimension cloud controller with 2 input variables.

Figure 18 shows the structure of the control system based on above controller.

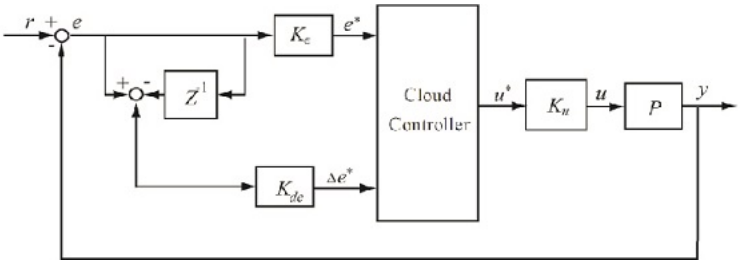

Figure 18: The structure of a control system based on two dimension cloud controller

Theorem 3.1 (Structure Decomposition Expression of Triangular Cloud Controller)**.** *A triangular cloud controller is decomposed with global nonlinear multi-value relay controller $u_G(k)$ and local nonlinear probability controller $u_L(k)$, that is,*

$$K_u \Delta u^*(k) = \Delta u_G(k) + \Delta u_L(k). \tag{5}$$

Proof. Suppose that the error $e(k)$ and error derivative $\Delta e(k)$ of set value and output are the inputs of the cloud controller. And also e^* and Δe^* are the values corresponding to $e(k)$ and $\Delta e(k)$after scaling. K_e, K_{de} are scaling factor of e and Δe, and K_u is proportionality factor, and r is set value.

$e^* = K_e e(k) = K_e(r - y(k))$, $\Delta e^* = K_{de}\Delta e(k) = K_{de}(e(k) - e(k-1))$, $e^* \in [-L, L], \Delta e^* \in [-L, L]$, $\Delta u \in [-H, H]$.

Where H, L is positive integer and usually $H = L = 1$.

Design of cloud controller follows below steps.

(1) $e^*, \Delta e^*$ have $M = 2J + 1$ symmetric cloud variables each ; J variables are positive and other J variables are negative , and last is zero. (Figure 19)

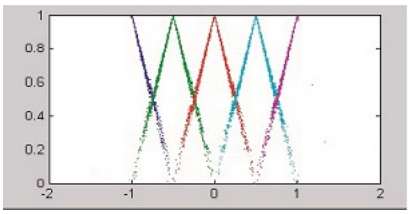

Figure 19: Symmetric premise membership cloud

Consider the Input variable $e^*, \Delta e^*$ are member of triangular membership cloud set E_i and ΔE_j,

$$\Delta E_j = (i, j = -J, -J+1, \cdots, -1, 0, 1, \cdots, J-1, J).$$

Each of μ_i and μ_j are the membership cloud function of e^* and Δe^*, and their expectation values are λ_i and λ_j each.

e^* and Δe^* take certain values in below interval

$$e^* \in [\lambda_i, \lambda_{i+1}], \Delta e^* \in [\lambda_i, \lambda_{i+1}].$$

where $-J+1 \le i, j \le J-1$. Then the triangular membership function width of e^* and Δe^* is as below.

$$En_e = \lambda_{i+1} - \lambda_i, En_{\Delta e} = \lambda_{j+1} - \lambda_j, (i, j = -J+1, \cdots, J-1).$$

So, the two dimension cloud model is as follows:

$$\begin{aligned}
\mu_i(e^*) &= (\lambda_{i+1} - e^*)/En_e^{'}, En_e^{'} = N(En_e, He_e) = \lambda_{i+1}^{'} - \lambda_i^{'} = N(\lambda_{i+1}, He_e) - N(\lambda_i, He_e), \\
\mu_{i+1}(e) &= 1 - \mu_i(e^*) = (e^* - \lambda_i)/En_e^{'}, \ \mu_j(\Delta e^*) = (\lambda_{j+1} - \Delta e^*)/En_{\Delta e}^{'}, En_{\Delta e}^{'} = N(En_{\Delta e}, He_{\Delta e}) \\
&= \lambda_{j+1}^{'} - \lambda_j^{'} = N(\lambda_{j+1}, He_{\Delta e}) - N(\lambda_j, He_{\Delta e}), \\
\mu_{j+1}(\Delta e) &= 1 - \mu_j(\Delta e^*) = (\Delta e^* - \lambda_j)/En_{\Delta e}^{'}.
\end{aligned}$$

where $N(\lambda_{i+1}, He)$ and $N(\lambda_i, He)$ means Gaussian distribution random number that the expectation value is λ_{i+1}, λ_i each, and their distribution is He.

The output variable Δu^* has equally distributed single point membership function. (Figure 20)

There are $2M-1$ (or $4J+1$) cloud variables that are represented as U_k.

where $k = -2J+1, -2J, \cdots, -1, 0, 1, \cdots, 2J-1, 2J$, $V = H/2J$, and the expectation value of U_k is $kV = kH/2J$.

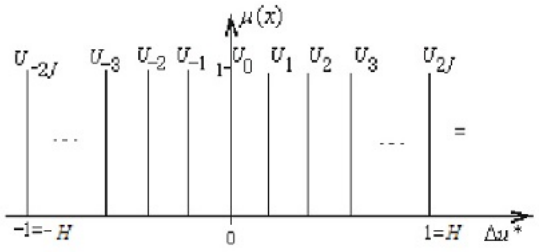

Figure 20: The Membership Cloud Function of Output variable Δu^*

(2) We can get M^2 possible combination of membership functions of e^* and Δe^* . And the control rules are as follows:

IF e^* is E_i and Δe^* is ΔE_j then Δu^* is $U_{-(i+j)}$

When e^* and Δe^* are known, among the M^2 rules, the only 4 membership cloud functions $\mu_i(e^*)$, $\mu_{i+1}(e^*)$, $\mu_j(\Delta e^*)$, $\mu_{j+1}(\Delta e^*)$ have values and others have zero value. The below 4 rules are fired.

Rule 1; IF e^* is E_i and Δe^* is ΔE_j then Δu^* is $U_{-(i+j)}$,

Rule 2; IF e^* is E_i and Δe^* is ΔE_{j+1} then Δu^* is $U_{-(i+j+1)}$,

Rule 3; IF e^* is E_{i+1} and Δe^* is ΔE_j then Δu^* is $U_{-(i+j+1)}$,

Rule 4; IF e^* is E_{i+1} and Δe^* is ΔE_{j+1} then Δu^* is $U_{-(i+j+2)}$.

(3) Design the cloud model projector.

Note the two dimension x condition cloud model of Rule 1 - Rule 4 as below.

Rule 1: $w_1^l = \mu_i(e^*) \cdot \mu_j(\Delta e^*) = ((\lambda_{i+1} - e^*)/En_e^{'})((\lambda_{j+1} - \Delta e^*)/En_{\Delta e}^{'})$,

Rule 2: $w_2^l = \mu_i(e^*) \cdot \mu_{j+1}(\Delta e^*) = ((\lambda_{i+1} - e^*)/En_e^{'})((\Delta e^* - \lambda_j)/En_{\Delta e}^{'})$,

Rule 3: $w_3^l = \mu_{i+1}(e^*) \cdot \mu_j(\Delta e^*) = ((e^* - \lambda_i)/En_e^{'})((\lambda_{j+1} - \Delta e^*)/En_{\Delta e}^{'})$,

Rule 4: $w_4^l = \mu_{i+1}(e^*) \cdot \mu_{j+1}(\Delta e^*) = ((e^* - \lambda_i)/En_e^{'})((\Delta e^* - \lambda_j)/En_{\Delta e}^{'})$.

(4) Generate the 1 dimension u consequent cloud.

Consequent triangular membership cloud function is determined as below equations. Let us assume the single membership cloud function is used and the membership function has the expectation value Ex_u , and its width and distribution is 0.

$$u_1 = Ex_{u,i+j} = \frac{-(i+j)}{2J}, \ u_2 = Ex_{u,i+j+1} = \frac{-(i+j+1)}{2J}, u_3 = Ex_{u,i+j+1} = \frac{-(i+j+1)}{2J}, \ u_4 = Ex_{u,i+j+2} = \frac{-(i+j+2)}{2J}.$$

As above two dimension x condition cloud model is a group of cloud drops, we use inverted cloud projector. Then the below total output is calculated by using center method.

$$u^*(k) = \frac{\sum_{h=1}^{4} w_h U_h}{\sum_{h=1}^{4} w_h} = \frac{w_1 \frac{-(i+j)}{2J} + w_2 \frac{-(i+j+1)}{2J} + w_3 \frac{-(i+j+1)}{2J} + w_4 \frac{-(i+j+2)}{2J}}{w_1 + w_2 + w_3 + w_4},$$

here,

$$\begin{aligned} w_1 + w_2 + w_3 + w_4 &= \mu_i(e^*) \cdot \mu_j(\Delta e^*) + \mu_i(e^*) \cdot \mu_{j+1}(\Delta e^*) + \mu_{i+1}(e^*) \cdot \mu_j(\Delta e^*) + \mu_{i+1}(e^*) \cdot \mu_{j+1}(\Delta e^*) \\ &= \mu_i(e^*) \cdot \mu_j(\Delta e^*) + \mu_i(e^*) \cdot (1 - \mu_j(\Delta e^*)) + \mu_{i+1}(e^*) \cdot \mu_j(\Delta e^*) + \mu_{i+1}(e^*) \cdot (1 - \mu_j(\Delta e^*)) \\ &= \mu_i(e^*) + \mu_{i+1}(e^*) = \mu_i(e^*) + (1 - \mu_i(e^*)) = 1. \end{aligned}$$

So, the final output of cloud controller is as follows:

$$\begin{aligned} u^*(k) &= w_1 \cdot \frac{-(i+j)}{2J} + w_2 \cdot \frac{-(i+j+1)}{2J} + w_3 \cdot \frac{-(i+j+1)}{2J} + w_4 \cdot \frac{-(i+j+2)}{2J} \\ &= (w_1 + w_2 + w_3 + w_4) \cdot \frac{-(i+j)}{2J} - w_2 \cdot \frac{1}{2J} - w_3 \cdot \frac{1}{2J} - w_4 \cdot \frac{2}{2J} \\ &= \frac{-(i+j)}{2J} - (w_1 + w_2 + w_3 + w_4) \cdot \frac{1}{2J} - w_4 \cdot \frac{1}{2J} + w_1 \cdot \frac{1}{2J} \\ &= -\frac{-(i+j)}{2J} - \frac{1}{2J} + w_1 \cdot \frac{1}{2J} - w_4 \cdot \frac{1}{2J} = -\frac{1}{2J}(i + j + 1 - w_1 + w_4) \\ &= -\frac{1}{M-1}(i+j+1) - \frac{1}{M-1}(w_4 - w_1). \end{aligned}$$

where, $w_1 = \mu_i(e^*) \cdot \mu_j(\Delta e^*), w_4 = (1 - \mu_i(e^*)) \cdot (1 - \mu_j(\Delta e^*))$ and $w_4 - w_1 = \frac{(2e^* - \lambda_i - \lambda_{i+1})}{N(\lambda_{i+1}, He) - N(\lambda_i, He)} \cdot \frac{(2\Delta e^* - \lambda_j - \lambda_{j+1})}{N(\lambda_{j+1}, He) - N(\lambda_j, He)}$

The output of cloud controller multiplied with proportional factor is represented as follows:

$$\begin{aligned} K_u \cdot u^*(k) &= -\frac{K_u}{M-1}(i+j+1) - \frac{K_u}{M-1}(w_4 - w_1) \\ &= -\frac{K_u}{M-1}(i+j+1) - \frac{K_u}{M-1}\left[\frac{(2e^* - \lambda_i - \lambda_{i+1})}{N(\lambda_{i+1}, He) - N(\lambda_i, He)} \cdot \frac{(2\Delta e^* - \lambda_j - \lambda_{j+1})}{N(\lambda_{j+1}, He) - N(\lambda_j, He)}\right]. \end{aligned} \tag{6}$$

As above equation, the cloud controller has 2 terms.

The first term is $-\frac{K_u}{(M-1)}(i+j+1)$ and represented as $u_G(k)$. Here, $e^* \geq 0, \Delta e^* \geq 0$. Then note $e^* \in [\lambda_i, \lambda_{i+1}], \Delta e^* \in [\lambda_j, \lambda_{j+1}]$, $i \geq 0$, and $j \geq 0$ are constant. So $\Delta u_G(k)$ is constant in the direct product space of interval $[\lambda_i, \lambda_{i+1}]$ and $[\lambda_j, \lambda_{j+1}]$. It changes when the intervals of e^* and Δe^* change. This means $\Delta u_G(k)$ has global multi-value relay characteristics.

$$\begin{aligned} \Delta u_L(k) &= \frac{-K_u}{(M-1)}\left[\frac{(2e^* - \lambda_i - \lambda_{i+1})}{N(\lambda_{i+1}, He) - N(\lambda_i, He)} \cdot \frac{(2\Delta e^* - \lambda_j - \lambda_{j+1})}{N(\lambda_{j+1}, He) - N(\lambda_j, He)}\right] \\ &= K_P\left(e^* - \frac{\lambda_i + \lambda_{i+1}}{2}\right) + K_D\left(\Delta e^* - \frac{\lambda_{j+1} + \lambda_j}{2}\right), \end{aligned}$$

where

$$K_P = -\frac{2K_u}{(M-1)(N(\lambda_{i+1}, He) - N(\lambda_i, He))}, \quad K_D = -\frac{2K_u}{(M-1)(N(\lambda_{j+1}, He) - N(\lambda_j, He))}.$$

As above equation, $\Delta u_L(k)$ is a PD controller with variable and stable statistical characteristic quantity which depends on e^* and Δe^* . And its proportion factor and differential coefficient are depends on the interval and the characteristic quantity in the interval. So note that this PD controller is a local controller.

It is demonstrated in the other cases of e^* and Δe^*

(end) □

4 Design of simple triangular cloud controller

In this section, the structure of the cloud controller, which does not use the mathematical model of the plant presented in the previous section, is very complex, and it is difficult to perform stability analysis of the closed cloud control system, so we design the simplest cloud controller structure by minimizing the design parameters of the cloud controller.

To do so, suppose that the positive domain of I/O variables is normalized from -1 to 1 and divided into three parts, and the key member cloud function is symmetric, uniformly divided triangle, the posterior member cloud function is a singleton cloud function, and the IO relation of cloud control rules is linear.

First, let us derive to the simple structure of cloud controller. The input variable cloud space is divided in 6 subspaces as shown in Figure 21.

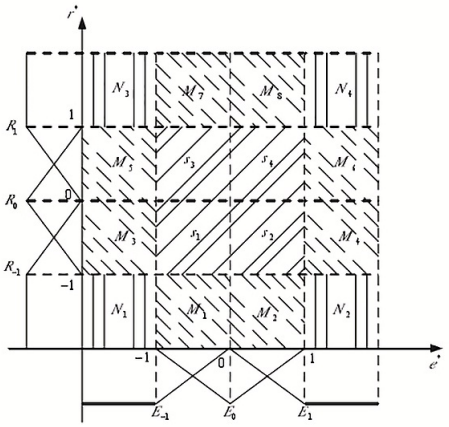

Figure 21: The input space of the cloud control system

In the subspaces- S_1, S_2, S_3, S_4 , 4 cloud rules are fired and in the subspaces - $M_1, M_2, \cdots, M_8$, 2 rules are fired and then 1 rule is fired in the subspaces N_1, N_2, N_3, N_4. If the rules are stable in maximum intersection space, they are stable in the whole space. So we consider the stability in S_1, S_2, S_3, S_4 of 14 subspaces.

In section 2, we derived the output of the cloud controller and it is as below.

$$u^*(k) = w_1 \cdot \frac{-(i+j)}{2J} + w_2 \cdot \frac{-(i+j+1)}{2J} + w_3 \cdot \frac{-(i+j+1)}{2J} + w_4 \cdot \frac{-(i+j+2)}{2J}$$
$$J = 1, i = j = -1, \lambda_{i+1} = \lambda_{j+1} = 0, \lambda_i = \lambda_j = -1.$$

from Fig. 21, $J = 1, i = j = -1, \lambda_{i+1} = \lambda_{j+1} = 0, \lambda_i = \lambda_j = -1$, finally in above equation $\frac{-(i+j+2)}{2J} = 0$.

$$\begin{aligned} u^*(k) &= w_1 \cdot \frac{-(i+j)}{2J} + w_2 \cdot \frac{-(i+j+1)}{2J} + w_3 \cdot \frac{-(i+j+1)}{2J} \\ &= \frac{(\lambda_{i+1} - e^*)}{N(\lambda_{i+1}, He) - N(\lambda_i, He)} \cdot \frac{(\lambda_{j+1} - \Delta e^*)}{N(\lambda_{j+1}, He) - N(\lambda_j, He)} \cdot \frac{-(-1-1)}{2} + \\ &\quad + \frac{(\lambda_{i+1} - e^*)}{N(\lambda_{i+1}, He) - N(\lambda_i, He)} \cdot \frac{(\Delta e^* - \lambda_j)}{N(\lambda_{j+1}, He) - N(\lambda_j, He)} \cdot \frac{-(-1-1+1)}{2} \\ &\quad + \frac{(e^* - \lambda_i)}{N(\lambda_{i+1}, He) - N(\lambda_i, He)} \cdot \frac{(\lambda_{j+1} - \Delta e^*)}{N(\lambda_{j+1}, He) - N(\lambda_j, He)} \cdot \frac{-(-1-1+1)}{2}. \end{aligned}$$

From Fig. 21,$\lambda_{i+1} = \lambda_{j+1} = 0, \lambda_i = \lambda_j = -1$, note that, $\lambda_{i+1} = \lambda_{j+1} = 0, \lambda_i = \lambda_j = -1$, $N(\lambda_{i+1}, He) - N(\lambda_i, He) \approx 1, N(\lambda_{j+1}, He) - N(\lambda_j, He) \approx 1$ therefore

$$u^*(k) = e^*\Delta e^* - \tfrac{1}{2}e^*(\Delta e^* + 1) - \tfrac{1}{2}\Delta e^*(e^* + 1) = e^*\Delta e^* - \tfrac{1}{2}e^*\Delta e^* - \tfrac{1}{2}e^* - \tfrac{1}{2}e^*\Delta e^* - \tfrac{1}{2}\Delta e^* = -\tfrac{1}{2}(e^* + \Delta e^*). \quad (7)$$

From the above, it can be seen that the triangular cloud controller without using the analytical model of the plant is represented by the structure of the PD controller in the simplest case.

5 Stability analysis of the triangular cloud control system

In this section, we discuss the stability analysis of closed-loop systems when the simplest triangular cloud controller discussed in the previous section is applied to the stabilization control of plants represented by nonlinear state equations. Note that the mathematical model of the plant represented by the nonlinear state equation presented here is only used to verify the stability analysis of the triangular cloud controller and when designing a real controller, we design the controller as a controller designed in Section 2 without using the mathematical model of the plant.

We present some theorems from previous studies.

Definition 5.1. [26] *Let the fuzzy system be represented as Eq. (8). The energy function satisfies Eq. (9) and* $x(t) \neq 0$. *When* $\dot{V}(x(t)) < 0$, $V(x(t))$ *is referred to as a Fuzzy Lyapunov Function of the fuzzy system Eq. (8).*

$$R^{\rho}: \text{ if } x_i \text{ is } A_1^{\rho} \text{ and } x_2 \text{ is } A_2^{\rho} \text{ and } \cdots x_n \text{ is } A_n^{\rho} \text{ then } \dot{x}(t) = A_{\rho}x(t) + B_{\rho}u(t). \tag{8}$$

$$V\left(x\left(t\right)\right) = x\left(t\right)^{T} P\left(x\left(t\right)\right) x\left(t\right), P\left(x\left(t\right)\right) = \sum_{\rho=1}^{r} h_{\rho}\left(x\left(t\right)\right) P_{\rho}, \rho = 1, 2, \cdots, r. \tag{9}$$

where P_{ρ} *is a positive definite symmetric matrix and* $h_{\rho}\left(x\left(t\right)\right)$ *is fitness of* ρ*th rule of the fuzzy system.*

Theorem 5.2. [26]

Assume that $\Phi_1, \Phi_2, \cdots, \Phi_r$ *satisfy* $\left|\dot{h}_{\rho}(x(t))\right| \leq \Phi_{\rho}$. *If*

$$P_i > 0, \quad \sum_{\rho=1}^{r} \Phi_{\rho} P_{\rho} + \frac{1}{2}(A_k^T P_k + P_k A_k + A_K^T P_i + P_i A_k) < 0, \quad k \leq i, \tag{10}$$

then T-S fuzzy system Eq. (8) is asymptotically stable.

The Lyapunov function based fuzzy controller design methods are generally classified into common positive definite symmetric matrix based method [26], piecewise continuous Lyapunov function family based method [30] and fuzzy Lyapunov function based method [14]. Here, fuzzy Lyapunov function based method is a combination of common positive definite symmetric matrix based method and piecewise continuous Lyapunov function family based method. And it is widely used in stability analysis. In this paper, we present the cloud Lyapunov function based method and analyze the stability.

The SISO nonlinear model of the plant is represented as Eq. 11.

$$\begin{cases} \dot{x} = A(x)x + B(x)u \\ y = C(x)x \end{cases} \tag{11}$$

where $x \in R^n$ is the state variable, $A(x), B(x), C(x)$ are parameter matrices each. They have certain dimension and represent the non-linearity of the system.

Let $r(t)$ be the set value of the system and the error of output. $e(t) := r(t) - y(t)$.

The control plant is $\lim_{t\to\infty} e(t) = 0$.

Let $x = x_0$ be the equilibrium point.

When $x = x_0 + \Delta x$, $u = u_0 + \Delta u$, $y = y_0 + \Delta y$,

Eq. (11) is as below equation.

$$\begin{cases} \dot{x}_0 + \Delta\dot{x} = A((x_0 + \Delta x))(x_0 + \Delta x) + B((x_0 + \Delta x))(u_0 + \Delta u) \\ y = (C(x_0 + \Delta x))(x_0 + \Delta x) \end{cases} \tag{12}$$

If the parameter matrices are as below,

$$\begin{aligned} A(x_0 + \Delta x) &= A_0 + \Delta A(x), \\ B(x_0 + \Delta x) &= B_0 + \Delta B(x), \\ C(x_0 + \Delta x) &= C_0 + \Delta C(x). \end{aligned}$$

Eq. (11) is expanded to Eq. (13).

$$\begin{cases} \dot{x}_0 + \Delta\dot{x} = [A_0 + \Delta A(x)](x_0 + \Delta x) + [B_0 + \Delta B(x)](u_0 + \Delta u) \\ y_0 + \Delta y = [C_0 + \Delta C(x)](x_0 + \Delta x) \end{cases} \tag{13}$$

The plant is to get $u = u_0, y = y_0$ which satisfies Eq. (14).

$$\begin{cases} \dot{x}_0 = A_0 x_0 + B_0 u_0 \\ y_0 = C_0 x_0 \end{cases} \tag{14}$$

From Eq. (13) and Eq. (14),

$$\begin{cases} \Delta\dot{x} = A_0\Delta x + B_0\Delta u + \Delta A(x)x + \Delta B(x)u \\ \Delta y = C_0\Delta x + \Delta C(x)x \end{cases} \tag{15}$$

Let $X(t) := \Delta x, U(t) := \Delta u$ and $y_0 = r(t)$. Then,

$$\begin{cases} \dot{X}(t) = A_0 X(t) + B_0 U(t) + \bar{D}w(t) \\ e(t) = C_0 X(t) + Ev(t) \end{cases} \tag{16}$$

where $\bar{D}w = \Delta A(x)x + \Delta B(x)u, Ev = \Delta C(x)x$, and $\bar{D}, E$ are known constant matrix and have certain dimensions. The control law of triangular cloud controller is represented as Eq. (17).

From Eq. (7) and consideration of proportion factor and scaling coefficients,

$$U(t) = -\frac{k_u}{2}\left[k_e e(t) + k_{\dot{e}}\dot{e}(t)\right]. \tag{17}$$

Where $k_e, k_{\dot{e}}$ are scaling coefficients of the cloud controller and k_u is proportion coefficient can generally be found as follows.

$e(t)$ and $\dot{e}(t)$ are both explicit general variables and their universe (i.e., range of variation) is a continuous closed interval on the real axis, and these are denoted by X and Y, respectively.

In the cloud controller, this universe must be transformed into an internal universe X' and Y' are explicit general variables $e(t)$ and $\dot{e}(t)$, which changes to e^* and Δe^* , whether continuous or discrete after universe transformation.

$$k_e = \frac{X'_{\max} - X'_{\min}}{X_{\max} - X_{\min}}, k_{\dot{e}} = \frac{Y'_{\max} - Y'_{\min}}{Y_{\max} - Y_{\min}}.$$

On the other hand, the proportionality coefficient K_u is expressed as the conversion coefficient from cloud variable space Z' to explicit ordinary variable space Z.

$$k_u = \frac{Z_{\max} - Z_{\min}}{Z'_{\max} - Z'_{\min}}.$$

Eq. (15) is expanded from Eq. (14) as Eq. (18).

$$\begin{aligned} U(t) &= -\frac{k_u}{2}\left\{k_e\left[C_0X(t) + Ev(t)\right] + k_{\dot{e}}\left[C_0\dot{X}(t) + E\dot{v}(t)\right]\right\} \\ &= -\frac{k_u k_e}{2}\left[C_0X(t) + Ev(t)\right] - \frac{k_u k_{\dot{e}}}{2}\left\{C_0\left[A_0X(t) + B_0U(t) + \bar{D}w(t)\right] + E\dot{v}(t)\right\}. \end{aligned}$$

$$U(t) = -k^*\left\{C_0\left(k_eI_n + k_{\dot{e}}A_0\right)X(t) + k_eEv(t) + k_{\dot{e}}\left[C_0\bar{D}w(t) + E\dot{v}(t)\right]\right\}, \tag{18}$$

where $k^* = 0.5k_u\left(1 + k_uk_{\dot{e}}C_0B_0/2\right)^{-1}$. From Eq. (16) and (17), the state space model of closed-loop cloud model controller system is represented as follows:

$$\begin{aligned} \dot{X}(t) &= A_0X(t) + B_0U(t) + \bar{D}w(t) \\ &= A_0X(t) + k^*B_0\{C_0\left(k_eI_n + k_{\dot{e}}A_0\right)X(t) + k_eEv(t) + k_{\dot{e}}\left[C_0\bar{D}w(t) + E\dot{v}(t)\right]\} + Dw(t) \\ &= \left[A_0 - k^*B_0C_0\left(k_eI_n + k_{\dot{e}}A_0\right)\right]X(t) + k^*k_eB_0Ev(t) + \left[k^*k_{\dot{e}}B_0C_0 + I_n\right]\bar{D}w(t) + k^*k_{\dot{e}}B_0E\dot{v}(t). \end{aligned}$$

$$\begin{cases} \dot{X}(t) = \bar{A}X(t) + D\omega(t) \\ e(t) = C_0X(t) + Ev(t) \end{cases} \tag{19}$$

where

$\bar{A} := A_0 - k^*B_0C_0\left(k_eI_n + k_{\dot{e}}A_0\right)$, $D := \begin{bmatrix} k^*k_eB_0E & (k^*k_{\dot{e}}B_0C_0 + I_n)\bar{D} & k^*k_{\dot{e}}B_0E \end{bmatrix}$, $\omega(t) := \begin{bmatrix} v^T(t) & w^T(t) & \dot{v}^T(t) \end{bmatrix}^T$

Definition 5.3. *If the output(Eq. (18)) of the cloud controller of the control system Eq. (19). satisfies:*
(1) *When $\omega(t) = 0$, control system is asymptotically stable.*
(2) *When $\omega(t) \neq 0$, given constant $\gamma > 0$ and $x(0) = x_0$ (zero initial condition), $||X(t)||^2 < \gamma^2 ||\omega(t)||^2$*

Then the cloud controller is referred as H_∞ cloud controller.

Theorem 5.4. *For the control system Eq. (19), assume that $\gamma > 0$ and $\left|\dot{h}_k(X(t))\right| \leq \phi_k$.*

If the positive definite symmetric matrices $P_l (l = 1, 2, 3, 4)$ satisfy the LMI inequality in the subspaces $S_j (j = 1, 2, 3, 4)$ shown in Fig. 6, then the cloud control system Eq. (19) is asymptotically stable and has the H_∞ performance index.

$$\sum_{k=1}^{4} \phi_k P_k + \bar{A}_l^T P_l + P_l \bar{A}_l + \frac{1}{\gamma} P_l D D^T P_l + \frac{1}{\gamma} C_0^T C_0 < 0. \tag{20}$$

Proof. Define the cloud Lyapunov function in the cloud model subspace S_1 as $V_1(X) = X^T(t) \sum_{l=1}^{4} h_l P_l X(t)$. Assume P_l is a positive definite symmetric matrix and $h_l = \frac{\mu_{R^l}(e)\mu_{R^l}(ec)}{\sum_{l=1}^{4} \mu_{R^l}(e)\mu_{R^l}(ec)}, l = 1, 2, 3, 4$. Then the derived function of the cloud Lyapunov function $V_1(X)$ is as follows:

$$\dot{V}_1(X) = X^T(t) \sum_{k=1}^{4} \dot{h}_k P_k X(t) + \sum_{l=1}^{4} h_l \left[\dot{X}^T(t) P_l X(t) + X^T(t) P_l \dot{X}(t) \right].$$

Let us define a nonlinear function as below.

$$H(X, \omega) = \dot{V}_1(X) + \frac{1}{\gamma} y^T(t) y(t) - \gamma \omega^T(t) \omega(t). \tag{21}$$

Consider the two cases when the outside disturbance of the system $\omega(t) = 0$, and $\omega(t) \neq 0$. In the first case - when $\omega(t) = 0$, $\left|\dot{h}_k\right| \leq \phi_k$. This leads to;

$$\dot{V}_1(X) = X^T(t) \sum_{k=1}^{4} \phi_k P_k X(t) + \sum_{l=1}^{4} h_l \left[\dot{X}^T(t) P_l X(t) + X^T(t) P_l \dot{X}(t) \right] = X^T(t) \sum_{l=1}^{4} h_l \left[\sum_{k=1}^{4} \phi_k P_k + \left(\bar{A}_l^T P_l + P_l \bar{A}_l \right) \right] X(t).$$

When $h_l > 0$ and $\sum_{k=1}^{4} \phi_k P_k + \bar{A}_l^T P_l + P_l \bar{A}_l < 0$, then $\dot{V}_1(X) < 0$, that is, the cloud control system Eq. (19) is stable.

In the second case - $\omega(t) \neq 0$,

$$\dot{V}_1(X) \leq X^T(t) \sum_{k=1}^{4} \phi_k P_k X(t) + \sum_{l=1}^{4} h_l \left[X^T(t) \left(\bar{A}_l^T P_l + P_l \bar{A}_l \right) X(t) + \omega^{\mathrm{T}}(t) D^T P_l x(t) + X^T(t) P_l D \omega(t) \right].$$

For the arbitrary certain dimension matrix X, Y, below equations are true.

$$X^T Y + Y^T X \leq \gamma X^T X + \frac{1}{\gamma} Y^T Y, \quad \forall \gamma > 0, \omega^T(t) D^T P_l X(t) + X^T(t) P_l D \omega(t) \leq \gamma \omega^T(t) \omega(t) + \frac{1}{\gamma} X^T(t) P_l D D^T P_l X(t).$$

So,

$$\dot{V}_1(X) \leq X^T(t) \sum_{k=1}^{4} \phi_k P_k X(t) + \sum_{l=1}^{4} h_l \left[X^T(t) \left(\bar{A}_l^T P_l + P_l \bar{A}_l + \tfrac{1}{\gamma} P_l D D^T P_l \right) X(t) + \gamma \omega^T(t) \omega(t) \right]. \tag{22}$$

And from Eq. (21) and Eq. (22) we can get Eq. (23),

$$\sum_{k=1}^{4} \phi_k P_k + \bar{A}_l^T P_l + P_l \bar{A}_l + \frac{1}{\gamma} P_l D D^T P_l + \frac{1}{\gamma} C_0^T C_0 < 0. \tag{23}$$

If Eq. (23) is satisfied, then $H(X, \omega) < 0$. Under the zero initial condition we can get Eq. (24) by integrating Eq. (19). From 0 to T.

$$\int_0^T \dot{V}_1(X) dt + \int_0^T \left[\frac{1}{\gamma} y^T(t) y(t) - \gamma \omega^T(t) \omega(t) \right] dt < 0. \tag{24}$$

When $T \to \infty$,

$$\int_0^\infty \left[\frac{1}{\gamma} y^T(t)y(t) - \gamma\omega^T(t)\omega(t)\right] dt < -\int_0^\infty \dot{V}_0(X)dt = -X^T P_l X < 0. \tag{25}$$

Thus,

$$\frac{1}{\gamma} y^T(t)y(t) < \gamma\omega^T(t)\omega(t), \|y(t)\|^2 < \gamma^2 \|\omega(t)\|^2 .$$

So, when $\omega(t) \neq 0$ and $\sum_{k=1}^{4} \phi_k P_k + \bar{A}_l^T P_l + P_l \bar{A}_l + \frac{1}{\gamma} P_l D D^T P_l + \frac{1}{\gamma} C_0^T C_0 < 0$, equality $H(X, \omega) < 0$ is true and the cloud control system is stable in the subspace S_1 and has the H_∞ control performance index - γ.

To get the same result not only in S_1 but also in S_2, S_3, S_4 , assume that $P = \sum_{j=1}^{4} \lambda_j P_j$. And let us define the global Lyapunov function as following:

$$V(X(t)) = X^T(t)PX(t) = X^T(t) \sum_{j=1}^{4} \sum_{l=1}^{4} \lambda_j h_l P_l X(t) = \sum_{j=1}^{4} \lambda_j X^T(t) \sum_{l=1}^{4} h_l P_l X(t) = \sum_{j=1}^{4} \lambda_j V_j(X(t)).$$

Now, if $V_j, j = 1, 2, 3, 4$ are positive definite symmetric matrices and satisfy Theorem 5.4, then the derivative function of the Lyapunov function is negative and the cloud control system is asymptomatically stable in the whole input space. $V(X(t))$.

(End) □

Fig. 22 shows the block diagram of the designed cloud control system.

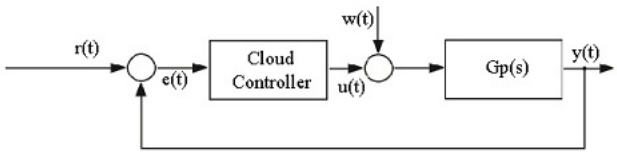

Figure 22: Block diagram of the cloud control system

The stability analysis procedure of the closed-loop cloud control system is as follows:

Step 1. Derive the analytic structure of the cloud control system and obtain the I/O relation equation.

Step 2. If the cloud control system can be represented as a linear function, transform into a state space equation. Else if it is represented as a nonlinear function, convert into linear differential equation by the Tayler expansion and transform it into a state space equation.

Step 3. Find out the subspaces of the maximum intersecting rule couples and prove the stability of the system in the subspaces.

Step 4. Set γ and determine the positive definite symmetric matrices P_l which satisfies the LMI inequality.

Step 5. Prove the stability of the closed-loop cloud control system on the result in Step 4.

6 Simulation

As an example of stability analysis of the cloud controller, we consider the stabilization control of a straight line inverted pendulum on a cart [15], a typical experimental instrument.

The motion equation of the inverted pendulum is as follows:

$$\begin{aligned} \dot{x}_1(t) &= x_2(t) \\ \dot{x}_2(t) &= \frac{g\sin(x_1(t)) - aml x_2^2(t)\sin(2x_1(t))/2 - a\cos(x_1(t))u(t)}{4l/3 - aml\cos^2(x_1(t))} \end{aligned} \tag{26}$$

where x_1 is the inclined degree,$x_2$is the angular speed and $2l$ is the length of the pendulum, M is the mass of the cart, a is the equivalent amplification factor, $m$is the mass of the pendulum, u is the voltage of the electric motor,

$x_1 = \theta$, $x_2 = \omega = \dot{\theta}$, $g = 9.8m/s^2, m = 2Kg, M = 8Kg$, $l = 0.3m, a = 1/(m + M)$.

Using Eq. (26) as the state-space model, we have

$$\begin{array}{l} \left[\begin{array}{c} \dot{x}_1(t) \\ \dot{x}_2(t) \end{array}\right] = \left[\begin{array}{cc} 0 & 1 \\ \frac{g\sin(x_1(t))}{4l/3-aml\cos^2(x_1(t))} & -\frac{amlx_2^2(t)\sin(2x_1(t)/2}{4l/3-aml\cos^2(x_1(t))} \end{array}\right] + \left[\begin{array}{c} 0 \\ \frac{-a\cos(x_1(t)))}{4l/3-aml\cos^2(x_1(t))} \end{array}\right] u(t), \\ y(t) = [1 \quad 0] \left[\begin{array}{c} x_1(t) \\ x_2(t) \end{array}\right]. \end{array} \tag{27}$$

By setting $X = [x_1 x_2]^T$, $X = X_0 + \Delta X$ in Eq.(27) and linearizing around zero of state $x_1(t)$, the linear state space model is obtained as follows :

$$\begin{array}{l} \dot{X}_0(t) = A_0 X_0(t) + B_0 u(t), \\ y_0(t) = C_0 X_0(t). \end{array} \tag{28}$$

$$A_0 = \left[\begin{array}{cc} 0 & 1 \\ \frac{g}{4l/3-aml} & 0 \end{array}\right], B_0 = \left[\begin{array}{c} 0 \\ \frac{-a}{4l/3-aml} \end{array}\right], C_0 = [1 \ 0].$$

Considering Eq. (28) in Eq. (27), we have

$$\begin{array}{l} \dot{X}(t) = A_0 X(t) + B_0 u(t) + \bar{D} w(t), \\ y(t) = C_0 X(t). \end{array} \tag{29}$$

$$\bar{D} w(t) = \Delta A X(t) + \Delta B u(t).$$

$\bar{D}$ is $2 * 1$-dimensional known matrix.

Cloud scaling factor and proportionality factor for the above plant designed as follows.

$$k_e = \frac{1-(-1)}{\pi/2-(-\pi/2)} \approx 0.64, \ k_{\dot{e}} = \frac{1-(-1)}{\pi-(-\pi)} \approx 0.32, \ k_u = \frac{5-(-5)}{1-(-1)} = 5.$$

Substituting the control force obtained by Eq. (17) into Eq. (29), the following equation of state of the closed-loop cloud control system is obtained:

$$\begin{array}{l} \dot{X}(t) = \bar{A} X(t) + B_0 u(t) + D w(t), \\ y(t) = C_0 X(t). \end{array} \tag{30}$$

$$\bar{A} := A_0 - k^* B_0 C_0 \left(k_e I_n + k_{\dot{e}} A_0\right), \ D := \left[\begin{array}{cc} k^* k_e B_0 E & (k^* k_{\dot{e}} B_0 C_0 + I_n)\bar{D} \ k^* k_{\dot{e}} B_0 E \end{array}\right], \ w(t) := w(t)$$

Substituting the plant physical parameters and controller parameters, the scaling factor and the proportionality factor of the cloud controller in Eq. (30), the state equations of the closed-loop cloud control system are as follows (the parameters of the cloud controller are set as in Sections 2 and 3).

$$\begin{array}{l} \left[\begin{array}{c} \dot{x}_1(t) \\ \dot{x}_2(t) \end{array}\right] = \left[\begin{array}{c} 01 \\ 58.1 - 0.193 \end{array}\right] \left[\begin{array}{c} x_1(t) \\ x_2(t) \end{array}\right] + \left[\begin{array}{c} 0 \\ -0.255 \end{array}\right] w(t), \\ y(t) = [10] \left[\begin{array}{c} x_1(t) \\ x_2(t) \end{array}\right]. \end{array}$$

When $\phi_k = 0.4 (k = 1, 2, 3, 4), \gamma = 3$, the positive definite Lyapunov matrix satisfying the inequality condition (20) in Theorem 5.4.

$$P_1 = \left[\begin{array}{cc} 5.7838 & 0.9475 \\ 0.9475 & 8.4630 \end{array}\right], P_2 = \left[\begin{array}{cc} 3.5593 & 0.6051 \\ 0.6051 & 5.2080 \end{array}\right], P_3 = \left[\begin{array}{cc} 4.0042 & 0.6808 \\ 0.6808 & 5.8590 \end{array}\right], P_4 = \left[\begin{array}{cc} 4.8940 & 0.8321 \\ 0.8321 & 7.1610 \end{array}\right].$$

As can be seen from the above expression, the obtained Lyapunov matrices are positive definite symmetric matrices, so that the designed cloud control system is asymptotically stable.

The results of the electrode lifting control of the UHP furnace according to the Eq. (27) are shown in Fig. 23.

As shown in the figure, the simulation of the control with uncertainty in the presence of Gaussian white noise in the model of the electrode lifting control plant in the ultra-high power furnace shows that the fuzzy controller lacks uncertainty throughput, and the cloud controller has uncertainty throughput, and the proposed cloud controller has almost the same control effect as the Gaussian cloud controller.

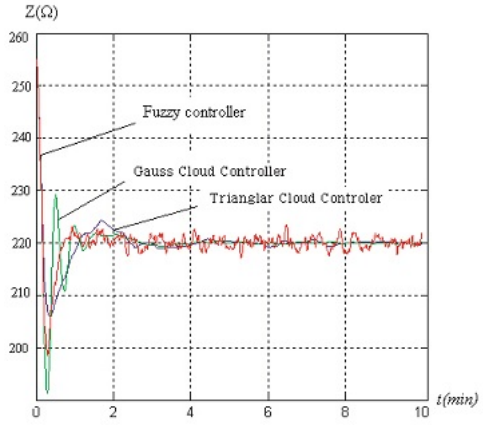

Figure 23: The simulation result of three methods of electrode lifting control of the UHP furnace

7 Conclusions

In this paper, we propose a method to design an asymmetric triangular cloud model controller that provides the stability of the system without using an analytical model of the plant.

The controller design method using the preceding cloud model uses the Gaussian membership cloud and its inference method to design the controller, and the resulting controller structure is a combination of exponential and logarithmic functions, which makes it difficult to decompose the controller structure as a nonlinear operation, and the stability analysis of the closed-cloud control system has not been studied.

To overcome the shortcomings of the controller design method with Gaussian membership cloud, a new asymmetric triangular membership cloud consisting of linear operations and its inference method is proposed and a controller design method based on it is developed.

In order to compare the previous fuzzy reasoning, the Gaussian membership cloud reasoning, and the proposed triangular membership cloud reasoning, computer simulations were carried out by applying the above reasoning methods to the problem of approximating the nonlinear function, and in the absence of uncertainty, three reasoning methods proved to similar results, In the presence of uncertainty, the proposed method proved to be superior to previous methods.

Next, we propose a controller design method using this model and show that an asymmetric triangular cloud controller that does not use an analytical model of the plant is applied to electrod up-down PID control of the UHP electric arc furnace, and the proposed controller has higher uncertainty throughput compared to fuzzy PID control through computer simulation.

To demonstrate that the proposed controller can analyze the stability of the closed-loop system even if no analytical model of the plant is given, we decompose the proposed controller structure and demonstrate that the structure of the triangular cloud controller is represented by a sum of nonlinear controllers with global multivalued relay characteristics and controllers with local nonlinear Next, the simplest cloud controller is designed and a closed-loop control system consisting of this controller and control plant is constructed to perform stability analysis, which is verified through the stabilizing control simulation of the inverted pendulum.

In conclusion, in the proposed asymmetric triangular cloud controller design, the analytical plant model is not used, and only the plant model is represented and demonstrated by an uncertain nonlinear model when the stability of the closed-loop cloud control system is analytically verified.

Future work is to propose a controller design method using the T-S cloud model and analyze its stability, given the analytical model of the plant.

Acknowledgement

The authors wish to express their appreciation for several excellent suggestions for improvements in this paper made by the referees.

References

[1] M. Aghase Yedabdollah, et al., *Supervised adaptive interval type-2 fuzzzy sliding mode control for planar cable-driven parallet-robots using Grosshopper*, Iranian Journal of Fuzzy Systems, **19**(5) (2022), 111-129.

[2] T. Allahviranloo, R. Saneifard, *Defuzzification method for ranking fuzzy numbers based on center of gravity*, Iranian Journal of Fuzzy Systems, **9**(6) (2012), 57-67.

[3] M. H. Asemani, *Non-pdc observer-based T-S fuzzy controller design and its application in chaos control*, Asian Journal of Control, **19** (2017), 969-982.

[4] J. Benic, M. Krznar, T. Stipancic, E. Situm, *A new concept of a fuzzy ontology controller for a temperature regulation*, Iranian Journal of Fuzzy Systems, **19**(4) (2022), 125-136.

[5] C. Y. Chen, *NN-based fuzzy control for TLP systems: A case study of practical structural parameters and wave properties*, Applied Soft Computing, **13** (2013), 755-763.

[6] C. H. Dai, Y. F. Zhu, *Adaptive probabilities of crossover and mutation in genetic algorithms based on cloud model*, Proceedings of 2006 IEEE, (2006), 710-713.

[7] V. Feliu-Batlle, R. Rivas-Perez, *Robust fractional-order controller for an EAF electrode position system*, Control Engineering Practice, Elsevier, **56** (2016), 159-173.

[8] G. Feng, *A survey on analysis and design of model-based fuzzy control systems*, IEEE Transactions on Fuzzy Systems, **14**(5) (2006), 676-697.

[9] M. Gani, M. A. Ullah, *Optimal PID tuning for controlling the temperature of electric arc furnace by genetic algorithm*, SN Applied Sciences, **880**(1) (2019), 1-8.

[10] Y. Guo, *Novel method of risk assessment based on cloud inference for natural gas pipelines*, Journal of Natural Gas Science and Engineering, **30** (2019), 421-429.

[11] R. He, J. Niu, et al, *A novel cloud-based trust model for pervasive computing*, Computer and Information Technology, CIT 04, The Fourth International Conference, (2004), 693-700.

[12] S. M. Hossein, M. Manthouri, *Type-2 adaptive fuzzy control approach applied to variable speed DFIG based wind turbines with WPPT algorithm*, Iranian Journal of Fuzzy Systems, **19**(1) (2022), 31-45.

[13] S. Kumar De, G. Chandra Mahata, *Decision of a fuzzy inventory with fuzzy backorder model under cloudy fuzzy demand rate*, International Journal of Applied and Computational Mathematics, Springer, **3**(3) (2017), 2593-2609.

[14] J. Lam, et al., *Dynamic output feedback H_∞ control of discrete time fuzzy systems: A fuzzy basis dependent lyapunov function approach*, International Journal of System Science, **38**(1) (2007), 25-37.

[15] D. Y. Li, *The pendulum control method and dynamic balance mode*, Chinese Engineering College, **4** (1999), 41-48.

[16] D. Y. Li, *A new cognitive model: Cloud model*, International Journal of Intelligent Systems, **24** (2009), 357-375.

[17] D. Y. Li, D. W. Cheng, et al, *Uncertainty reasoning based on cloud models in controllers*, Journal of Computer Science and Mathematics with Applications, **35** (1998), 99-123.

[18] D. Y. Li, H. Meng, *Membership clouds and membership clouds generator*, Computer Science - Research and Development, **32** (1995), 15-20.

[19] L. Maciel, *A fuzzy inference system modeling approach for interval-valued symbolic data forecasting*, Asian Journal of Control, **164** (2019), 1-250.

[20] J. M. Mendel, *Type-2 fuzzy sets: Some questions and answers*, IEEE Connections, Newsl. IEEE Neural Netw, **1** (2003), 10-13.

[21] J. M. Mendel, et al, *Type-2 fuzzy sets made simple*, IEEE Transactions on Fuzzy Systems, **10** (2002), 117-127.

[22] H. Mitchell, *Ranking type-2 fuzzy numbers*, IEEE Transactions on Fuzzy Systems, **14** (2006), 287-294.

[23] S. Mity, S. Kumar De, S. P. Mondal, *A study of a backorder EOQ model for cloud type intuitionistic dense fuzzy demand rate*, International Journal Fuzzy Systems, Springer, **22**(1) (2019), 201-211.

[24] M. Mizumoto, et al, *Some properties of fuzzy sets of type-2*, Information and Control, **31** (1976), 312-340.

[25] E. Segredo, C. Segura, C. Leon, E. Hart, *A fuzzy logic controller applied to a diversity-based multi-objective evolutionary algorithm for single-objective optimization*, Soft Computing, **19** (2015), 2927-2945.

[26] K. Tanaka, et al., *Fuzzy control system design and analyses: LMI Approach*, John Wiley and Sons, (2001), 52-57.

[27] M. Wang, *A compound cloud model for harmoniousness assessment of water allocation*, Environmental Earth Sciences, **75** (2016), 977-989.

[28] C. H. Wang, D. Y. Huang, *A new intelligent fuzzy controller for nonlinear hysteretic electronic throttle in modern intelligent automobiles*, IEEE Transactions on Industrial Electronic, **60**(6) (2013), 2332-2345.

[29] Y. J. Wang, Z. Y. Zhu, *Time series clustering based on shape dynamic time warping using cloud models*, Proceedings of the Second International Conference on Machine Learning and Cybernetics, **1** (2003), 236-241.

[30] H. Wango, H_∞ *controller design for affine fuzzy systems based on piecewise lyapunov functions in finite frequency domain*, Fuzzy Sets and System, Elsevier, **290** (2016), 22-38.

[31] D. Wu, W. Tan, *Type-2 FLS modeling capability analysis*, Proceedings of the FUZZ-IEEE, (2005), 242-247.

[32] L. A. Zadeh, *Fuzzy sets*, Information and Control, (1965), 338-353.

[33] F. Zhang, *Intelligence control based on membership cloud generator*, An Aviation Gazette, **20** (1999), 89-93.

[34] W. Zhengwu, *Robust decentralized adaptive fuzzy control of large-scale no affine nonlinear systems with strong interconnection and application to automated highway systems*, Asian Journal of Control, **21** (2019), 2387-2394.

[35] M. Zhu, A. Hahn, et al, *Identification-based controller design using cloud model for course-keeping of ships in waves*, Engineering Applications of Artificial intelligence, **175** (2018), 22-35 .